Generation of a poor prognostic chronic lymphocytic leukemia-like disease model: PKCα subversion induces an upregulation of PKCβII expression in B lymphocytes

Rinako Nakagawa[*,1,2], Milica Vukovic[*,1,3], Anuradha Tarafdar[1], Emilio Cosimo[1], Karen Dunn[1], Alison M. McCaig[1], Ailsa Holroyd[1], Fabienne McClanahan[4], Alan G. Ramsay[5], John G. Gribben[4] and Alison M. Michie[1,†]

[1]Institute of Cancer Sciences, College of Medical, Veterinary & Life Sciences, University of Glasgow, Glasgow, UK;
[2]The Babraham Institute, Cambridge, UK;
[3]MRC Centre for Regenerative Medicine, University of Edinburgh, Edinburgh, UK;
[4]Centre for Haemato-Oncology, Barts Cancer Institute, Queen Mary University of London, UK;
[5]Department of Haemato-Oncology, King's College London, UK.

[*]RN and MV contributed equally to this manuscript.

Running Title: Reduced PKCα induces progressive CLL-like disease

[†] *Corresponding author*: Alison M. Michie, Paul O'Gorman Leukaemia Research Centre, Gartnavel General Hospital, 21 Shelley Road, Glasgow G12 0XB; E-mail: Alison.Michie@glasgow.ac.uk; Tel: +44 (0)141 301 7885; Fax: +44 (0)141 301 7898.

Word Count: Abstract = 193 words; Text = 3972 words; 1 Table; 6 figures; 1 supplemental file

Acknowledgments: The authors would like to thank Odette Middleton for critically reviewing the manuscript. This work was funded by an MRC new investigator research grant (Ref: G0601099), and MRC/AstraZeneca project grant (Ref: MR/K014854/1) and an LLR project grant (Ref. 13012). MV was supported by a Lady Tata Memorial Trust Award, AMMcC was supported by an MRC Clinical Research Training Fellowship and flow cytometry facility was supported by KKLF (KKL501). We would like to thank Lilly and Co., for providing enzastaurin.

Abstract:

Overwhelming evidence identifies the microenvironment as a critical factor in the development and progression of chronic lymphocytic leukemia, underlining the importance of developing suitable translational models to study the pathogenesis of the disease. We previously established that stable expression of kinase dead protein kinase C alpha in hematopoietic progenitor cells resulted in the development of a chronic lymphocytic leukemia-like disease in mice. Here we demonstrate that this chronic lymphocytic leukemia model resembles the more aggressive subset of chronic lymphocytic leukemia, expressing predominantly unmutated immunoglobulin heavy chain genes, upregulated tyrosine kinase ZAP-70 expression and elevated ERK-MAPK-mTor signaling, resulting in enhanced proliferation and increased tumor load in the lymphoid organs. Reduced function of PKCα leads to an upregulation of PKCβII expression, which is also associated with a poor prognostic subset of human chronic lymphocytic leukemia samples. Treatment of chronic lymphocytic leukemia-like cells with the selective PKCβ inhibitor enzastaurin caused cell cycle arrest and apoptosis both *in vitro* and *in vivo*, and a reduction in the leukemic burden *in vivo*. These results demonstrate the importance of PKCβII in chronic lymphocytic leukemia-like disease progression and suggest a role for PKCα subversion in creating permissive conditions for leukemogenesis.

Key words: PKCα, chronic lymphocytic leukemia, mouse model, PKCβII

Introduction:

Chronic lymphocytic leukemia (CLL) is the most common leukemia in the Western world and is characterized by the presence of long-lived mature B cells with the distinct phenotype $CD19^{+}CD5^{+}CD23^{+}IgM^{lo}FMC7^{-}$.[1] Although deregulation of anti-apoptotic Bcl-2 family members indicated that CLL developed due to inappropriate accumulation of monoclonal B cells,[1,2] assessment of cell turnover revealed that CLL cells also undergo enhanced cell division within proliferation centers of lymphoid organs. This occurs through CLL cell interaction with the stromal niche, antigen and co-stimulation by activated $CD4^{+}$ T lymphocytes expressing CD40 ligand (CD40L), and interleukin 4 (IL4).[3-5] Therefore, CLL is a dynamic disease with significant rates of proliferation and death that requires complex *in vitro* and *in vivo* disease model systems to gain a fundamental understanding of the disease and design suitable therapies.

Clinically, CLL is a heterogeneous disease that can follow an indolent or aggressive course. Over the past decade it has been established that two major prognostic subtypes of CLL can be defined by the mutational status of the variable region of immunoglobulin heavy chain gene (IgV_H). Favorable outcomes are associated with expression of mutated (M) IgV_H genes, while cases harboring unmutated (UM) IgV_H genes, which can also express the tyrosine kinase, zeta-associated protein 70 (ZAP-70) and CD38, display more aggressive disease and frequently require therapeutic intervention.[6,7] ZAP-70 expression correlates highly with unmutated IgV_H.[8]

While a wealth of research into the biology of CLL has shown the importance of a number of proteins, particularly in those assisting in chemoresistance (eg., Mcl-1, absence of p53), no single genetic event has been linked to the initiation of CLL. Due to the heterogeneity within CLL, it is likely that a number of *in vitro* and *in vivo* models will be required to elucidate different aspects of the disease and gain a fuller understanding of the initiation, maintenance and progression of CLL. We previously demonstrated that retroviral-transduction of hematopoietic progenitor cells (HPCs) with a kinase dead PKCα construct (PKCα-KR) and subsequent culture either in an *in vitro* B cell generation culture (OP9 co-culture) or *in vivo*, resulted in the generation of CLL-like cells and disease,[9] indicating that modulation of PKCα function may play a role in CLL cell development. In the present study, we further characterize the

disease generated upon expression of PKCα-KR in HPCs and demonstrate that the CLL-like disease phenotypically resembles poor prognosis CLL.[1] Dissemination of CLL-like cells occurs in lymphoid organs with abnormal distribution in the spleens, and increased CLL-like cells in lymphoid organs, compared with control HPCs. In addition, the CLL-like cells exhibit limited/no somatic hypermutation in IgV_H genes, an upregulation of ZAP-70 expression and increased PKCβII expression accompanying disease maturation, which may account for the proliferation/survival advantage of these cells.[9] Selective targeting of PKCβ activity with enzastaurin resulted in the induction of cell cycle arrest and apoptosis *in vitro* and *in vivo*.

Methods:

Animals and Cells. Wildtype ICR and C57BL/6 mice were purchased from Harlan Laboratories Ltd. (Oxon, UK), and recombinase activating gene-1-deficient (RAG-$1^{-/-}$) mice were bred and maintained in-house at the University of Glasgow Central Research Facilities (Glasgow, UK). Splenic cell suspensions were generated from aged TCL-1 mice with manifest leukemia (12 month old Eμ-TCL-1 mice) maintained in Queen Mary University of London animal facility.[10] Timed-pregnant ICR or C57BL/6 mice were generated and fetal liver (FL) extracted at E14. Animals were maintained under standard animal house conditions in accordance with local and Home Office regulations. Peripheral blood samples were obtained, after informed consent, from patients with a clinically confirmed diagnosis of CLL (*Online Supplementary Table S1*). The studies were approved by the West of Scotland Research Ethics Service, NHS Greater Glasgow and Clyde, UK. CLL lymphocytes were isolated as previously described.[11] Normal peripheral blood samples were obtained, after informed consent, from buffy coats of healthy donors and B lymphocytes were separated with MACS human CD19 MicroBeads (Miltenyi Biotec Ltd., Surrey, UK). Leukemic B cells were purified from mouse spleens with MACS mouse CD19 MicroBeads (Miltenyi Biotec Ltd.). GP+E.86 packaging cells produce retrovirus encoding GFP alone (MIEV-empty vector control) or dominant negative PKCα (PKCα-KR).[12]

In vitro or in vivo B cell generation. HPCs isolated from E14 FL were prepared and retrovirally-transduced as described previously.[13] Retrovirally-transduced HPCs were cultured on a layer of OP9 cells for B cell development in the presence of IL-7 (Peprotech EC Ltd., London, UK), or adoptively transferred as described previously.[13] Mice were sacrificed between 5 to 8 wk post-injection and the bone marrow (BM), spleen, lymph node (LN) and blood were collected for analyses.

Flow Cytometric Analysis. Antibodies were purchased from BD Biosciences (Oxford, UK). Biotin-conjugated antibodies were detected by streptavidin-pacific blue (Invitrogen, Paisley UK). Single cell suspensions were stained as described previously.[13] The cells were acquired on a FACSCantoII (BD Biosciences) using the FACSDiva software package (BD Biosciences) and FlowJo software package (Tree

Star Inc, Ashland, OR, USA) to analyze the data. All data shown were lymphocyte gated by size and hematopoietic lineage gated by CD45 positive cells. Detailed methods are available in the *Online Supplement*.

Histology and immunohistochemistry. Spleens were collected from HPC-reconstituted mice and control RAG-1$^{-/-}$ mice after 5 wk and fixed in neutral buffered formalin (Sigma-Aldrich) at 4°C overnight and paraffin embedded following a standard ethanol and xylene protocol. Tissue sections were scanned with SlidePath Digital Pathology Solutions system (Leica Microsystems Ltd., Milton Keynes, UK). Detailed methods are available in the *Online Supplement.*

Cell cycle, apoptosis and proliferation analysis. Cell cycle was analyzed by detecting DNA content, visualized with propidium iodide (PI) intercalation as described previously.[9] BrdU incorporation assay was performed using Cell Proliferation Elisa BrdU kit (Roche Diagnostics, West Sussex, UK), following the manufacturer's protocol. Apoptosis was determined by analyzing Annexin V/DAPI staining (BD Biosciences), as previously described.[11]

Determine the mutational status of $IgV_{H.}$ C57BL/6 FL-derived HPCs were prepared, retrovirally-transduced and transferred into RAG-1$^{-/-}$ mice with C57BL/6 derived thymocytes. Mice were sacrificed at 5 wk post-injection and GFP^{+} splenic cells were prepared for sequencing of IgV_H regions. Detailed methods are available in the *Online Supplement*. The acquired data were analyzed using IMGT (www.imgt.org).

Western blots. MIEV- or PKCα-KR-HPC-co-cultures were removed from the OP9 layer and placed on plastic in complete medium for 2 hr to separate cells from adherent OP9 cells. Protein lysates were prepared and western blotting was performed as detailed in the *Online Supplement*. Blots were imaged with the Molecular Imager® ChemiDoc™ XRS system (Bio-Rad Laboratories, Hempstead, UK).

Quantitative real-time PCR. Quantitative real-time PCR was performed in triplicate with the 7900HT Fast Real-Time PCR system (Applied Biosystems, Warrington, UK) using the Taqman® Gene Expression Assay probe and primer set, and analyzed on

the ABI Prism 7900HT (Applied Biosystems) for mouse *prkcb* and *aicda,* with *gapdh* as a reference gene, as described previously.[11]

In vitro and in vivo drug treatment. In vitro MIEV- or PKCα-KR-HPC-co-cultures were removed from OP9 layer and density-centrifuged with Lympholyte-Mammal to remove dead cells. $1x10^6$ cells were treated with enzastaurin (LY317615, a gift from Eli Lilly) as indicated. Dimethyl sulfoxide (DMSO) was added as a vehicle no drug control (NDC). For *in vivo* studies, CLL-like disease was generated in mice as described above. Mice with confirmed leukaemia ($\geq$ 0.4% GFP^+CD19^+ in the blood), were treated with 75 mg/kg enzastaurin or vehicle (5% dextrose in water; D5W), twice a day for up to 21 days by oral gavage and then sacrificed for analyses.

Results:

Infiltration of CLL-like cells in the lymphoid organs of mice adoptively transferred with PKCα-KR-expressing HPCs. We have previously shown that PKCα-KR expression in wild type mouse HPCs, and subsequent culture in an *in vitro* B cell generating environment (HPC-OP9 co-culture) leads to the generation of cells phenotypically similar to human CLL ($CD19^+CD23^+CD5^+sIgM^{lo}$; Figure 1*A*;[9]). During the *in vitro* development of B cells, an upregulation of the mature B lineage marker CD23 is evident on both MIEV- and PKCα-KR-expressing cells by d10 of co-culture, with significantly higher expression noted on PKCα-KR-expressing cells (Figure 1*B*). CD23 expression was not accompanied by IgM upregulation, but instead was associated with higher expression of CD5 in PKCα-KR-expressing cells (Figure 1*C*). Moreover, the percentage of the $CD19^+CD5^+$ population increased significantly during the PKCα-KR cultures, while remaining unchanged in the MIEV cultures (*Online Supplementary Figure S1*).

Reconstitution of mice with an increasing number of PKCα-KR-HPCs (100K, 300K, 500K) significantly reduced mouse survival, with the majority of mice succumbing to a CLL-like disease between 6 – 9 weeks when reconstituted with 300K PKCα-KR-HPCs. As expected, reconstitution of mice with 500K MIEV-HPCs did not impact on survival (Figure 2*A*). Analysis of spleen size suggested an elevation in tumor load in PKCα-KR-HPC reconstituted mice, due to an elevation in spleen weight compared with MIEV-HPC and $RAG^{-/-}$ mice (Figure 2*B*). Analysis of the splenic architecture from MIEV- or PKCα-KR-HPCs reconstituted mice revealed the development of lymphoid follicular structures that were absent from the $RAG^{-/-}$ host spleen (Figure 2*C*). However PKCα-KR follicular cells were unusually distributed resulting in a disorganized splenic architecture, as indicated by H&E staining of splenic sections and immunohistochemistry staining for the B lineage marker B220, which co-stains with $CD19^+$ cells in both MIEV- and PKCα-KR-transduced cells (Figure 2*C*, *Online Supplementary Figure S2*). H&E staining also revealed lymphocyte infiltration in the liver of PKCα-KR mice, but not MIEV mice (*Online Supplementary Figure S3*). Flow cytometric analyses of retrovirally-transduced, GFP^+ cells that populate the lymphoid organs of reconstituted mice revealed a small population of $GFP^+CD19^+CD5^-$ B lineage cells in the BM, spleen and blood of MIEV-HPC mice. However, in PKCα-KR-HPC mouse organs and blood, the

majority of $CD19^+$ B cells were $CD5^+$, similar to CLL cells (Figures 2*D* & *E*). The percentage of $GFP^+CD19^+CD5^+$ B cells detected in blood, spleen, BM and LNs was significantly higher in PKCα-KR-mice compared with GFP^+CD19^+ MIEV control mice (Figure 2*E*). Moreover, the $GFP^+CD19^+CD5^+$ B cell population was detectable in blood at 3 weeks and increased over time (*Online Supplementary Figure S4*).

PKCα-KR transduced cells exhibit features of the poor prognostic subgroup of CLL patients. Examination of ZAP-70 expression levels by flow cytometry in *in vitro*-generated $CD19^+$ B cells and splenic B cells isolated from PKCα-KR-HPC mice revealed that PKCα-KR-expressing cells upregulated ZAP-70 expression compared to the control B cells and the established CLL mouse model Eμ-TCL-1 (Figures 3*A* & 3*B*). Low level ZAP-70 expression is observed in MIEV-expressing cells, which has previously been described in normal mature B cells (Figure 3*A*;[14]). Analysis of IgV_H mutational status revealed that the majority of PKCα-KR-expressing cells isolated from spleens exhibited unmutated IgV_H genes (6/8 sequences), compared with half (4/8 sequences) of the MIEV-expressing cells (Table 1). Interestingly, IgV_H genes from PKCα-KR-expressing cells contained longer CDR3 regions. Western blotting analysis revealed an activation of the ERK-MAPK and mTorc-1 pathways, as indicated by elevated phosphorylation of ERK1/2 and S6 in PKCα-KR cells (Figure 3*C*). Prolonged activation of the MEK/ERK pathway is associated with anti-apoptotic characteristics of CLL cells.[15] PKCα-KR cells also exhibited an elevated proliferative capacity compared with control B cells, both *in vitro* and *in vivo* (Figure 3*D* and 3*E*). Supporting this, *aicda* expression, which has been associated with increased CLL cell proliferation,[16,17] was significantly increased in GFP^+CD19^+ cells expressing PKCα-KR at the later stages of culture compared to MIEV-expressing cells (Figure 3*F*).

We previously demonstrated that PKCα-KR-transduced cells exhibited reduced PKC activity during the early stages of the OP9 co-culture, as expected (Figure 4*A*-left)[9]. However we observed an elevation in PKC activity later in the co-cultures at d17 compared to MIEV control (Figure 4*A*-right and *B*). As PKCβII upregulation has previously been associated with poor prognosis in CLL patients, we analyzed PKCβ expression.[18] Analysis of PKCα-KR-transduced cells revealed an upregulation of *prkcb* expression (*Online Supplementary Figure S5*) and an

upregulation of PKCβII protein expression in PKCα-KR-transduced cells compared with MIEV control cells, while PKCβI expression was unaltered (Figure 4*C*).

To determine the stage at which PKCβII is upregulated during the development of CLL-like cells on OP9 co-culture, MIEV- or PKCα-KR co-cultures were harvested as indicated and PKCβII expression was determined. PKCβII expression increased between d10 and d15 of co-culture in PKCα-KR-transduced cells, while remaining unchanged in MIEV control cells (Figure 4*D*). Upregulation of PKCβII and concomitant downregulation of PKCα expression has previously been shown in CLL patient samples,[18,19] a finding that was confirmed in our CLL cohort. Compared to peripheral blood B lymphocytes obtained from healthy volunteers, PKCα expression was barely detectable in the majority of CLL samples (12/16 samples), while PKCβII expression was elevated in half of the samples assessed (Figure 4*E*). Analysis of this cohort did not indicate an association of absent/low PKCα expression with a specific prognostic subgroup of CLL patients (*Online Supplementary Table S1*). PKCα expression was downregulated in B cells isolated from Eμ-TCL-1 spleens compared with age-matched wild type controls, however this did not reach statistical significance (Figure 4F). Interestingly PKCα expression was also downregulated in PKCα-KR-expressing splenic B cells. There was a trend towards upregulation of PKCβII expression in *in vivo* generated PKCα-KR B cells, however this was not observed in purified the Eμ-TCL-1 splenic B cells, which exhibited similar PKCβII expression to age-matched control B cells (Figure 4*F*). Analysis of the ERK-MAPK-mTor signaling pathway *in vivo* demonstrated a significant activation of mTor kinase, as indicated by the elevation in phosphorylated S6 both in PKCα-KR-expressing and Eμ-TCL-1 splenic B cells (Figure 4*G*). However, pERK exhibited variability between mice therefore not showing a clear upregulation in ERK-MAPK activity.

Taken together, our CLL-like cells exhibit a higher expression of markers associated with adverse outcome in CLL patients and possess an enhanced proliferation capacity, likely due to elevated mTor signaling upon PKCα subversion. This, coupled with the finding that PKCα expression is reduced in the majority of CLL patient samples assessed, indicates that our CLL-like disease model is a translationally-relevant model for the progressive human disease.

PKCβ selective inhibitors inhibit CLL-like cell proliferation in vitro and in vivo

To determine whether PKCβ plays an important role in driving proliferation and cell survival in our mouse CLL-like disease model *in vitro*, CLL-like cells were treated with the PKCβ selective inhibitor, enzastaurin. PKCβ has previously been shown to phosphorylate and inhibit GSK3β.[20] Therefore to test the selectivity of enzastaurin for PKCβ-mediated signals, we assessed the phosphorylation status of GSK3β. PKCα-KR-expressing cells from late co-cultures exhibited increased phospho-GSK3β^{S9}, which was abrogated by enzastaurin treatment (20 μM; Figure 5*A*). Enzastaurin treatment induced a selective and significant elevation in apoptosis above background (NDC) both in PKCα-KR-expressing cells (left) and splenic Eμ-TCL-1 cells (right) compared with control MIEV and aged C57Cl/6 cells respectively, as indicated by an elevation in the percentage of Annexin V$^+$DAPI$^-$ cells in the leukemic cells (Figure 5*B* and *Online Supplementary Figure S6*).

Analysis of the effect of enzastaurin treatment on cellular proliferation revealed a G_1 arrest in PKCα-KR-cultures only (Figure 5*C*-left). This was accompanied by a significant reduction in the proportion of cells undergoing mitosis in PKCα-KR-cultures (Figure 5*C*-right). Coupled with these data, enzastaurin treatment significantly reduced the BrdU incorporation of PKCα-KR cells at 24 and 48 hr (Figure 5*D*). In addition, and supporting the data presented in Figure 3*D*, PKCα-KR-expressing cells exhibited a significantly higher proliferation rate than MIEV cells in untreated cultures, and treatment of these cells with enzastaurin reduced their proliferation rate to that of MIEV cells (Figure 5*D*). These results demonstrate that enzastaurin selectively inhibited cell cycle progression and proliferation in CLL-like cells *in vitro*.

To test the efficacy of enzastaurin to inhibit proliferation of CLL-like cells *in vivo*, mice were treated with enzastaurin twice a day for up to three weeks, after confirmation that the mice were leukemic (≥ 0.4% GFP$^+$CD19$^+$CD5$^+$ cells in the blood). Enzastaurin treated mice displayed a decrease in the percentage and number of GFP$^+$CD19$^+$CD5$^+$ cells in the BM, spleen, LN and blood compared with vehicle-treated controls, reaching significance in the BM, spleen and blood (Figure 6*A* – 6*C*). Interestingly, a decrease in CLL-like cells in the blood was observed during treatment, although this did not reach significance. In addition, there was a significant induction

of apoptosis in enzastaurin treated CLL-like cells in both the BM and spleen, compared with vehicle-treated CLL cells (Figure 6*D*). Collectively, these results indicate that targeted therapies towards PKCβ-mediated signaling pathways show promise as potential therapies for progressive CLL, by impeding CLL cell proliferation and inducing apoptosis.

Discussion:

We previously established that subversion of PKCα confers a CLL-like phenotype to B lineage cells both *in vitro* and *in vivo*.[9] We now demonstrate that PKCα-KR-expressing CLL-like cells display poor prognostic features of the human disease both *in vitro* and *in vivo*, and aberrantly expand in lymphoid organs of mice *in vivo*. These CLL-like cells exhibit elevated proliferation, likely due to an activation of ERK-MAPK-mTor signaling, indicating that PKCα-KR-expressing cells display properties of progressive disease. Importantly, we demonstrate that PKCα expression is downregulated in the majority of CLL cases assessed indicating that this model is translationally relevant for the study of CLL. Subsequent to PKCα-KR expression we identified an elevation in PKCβII expression, a PKC isoform that has been implicated in CLL pathogenesis, which when inhibited with enzastaurin, reduced tumor load within the spleen, due to the induction of cell cycle arrest and apoptosis.

Expression patterns of specific PKC isoforms are deregulated in a number of cancers. PKCα is upregulated in breast, gastric, prostate and brain cancers, suggesting that it contributes to tumorigenesis,[21,22] and higher expression levels have been linked with the aggressiveness and invasive capacity of breast cancer cells.[23,24] However, PKCα expression is downregulated in epidermal, pancreatic, colon cancers[25-29] and CLL[18] suggesting that PKCα can also function as a tumor suppressor. This was demonstrated in mouse models for colon cancer, where a reduction in PKCα expression was observed in carcinogen-induced colon cancer,[29] and $APC^{min/+}$ mice.[30] Indeed, crossing $APC^{min/+}$ mice onto the $PKC\alpha^{-/-}$ background led to an accelerated, more aggressive development of colon cancer.[30,31] Interestingly, spontaneous development of cancerous lesions in the intestinal tract occurred with higher frequency in aging $PKC\alpha^{-/-}$ mice compared with littermate controls. The malignant cells within the lesions derived from $PKC\alpha^{-/-}$ mice possessed a higher mitotic index compared with those from littermate controls. Taken together, these data strongly suggest a role for PKCα in the regulation of cell division and suppression of tumor formation in selected cancers.[30] Of note, PKCβII upregulation has been intrinsically linked to the development of colon cancer.[29,32] Similarly, PKCβ has recently been shown to be essential for CLL development in the TCL-1 Tg CLL mouse model, with deletion of PKCβ in a murine model of CLL leading to an increase in survival.[33]

Surprisingly, we found that PKCβII expression remained unchanged in B lineage cells isolated from TCL-1 Tg splenic cells, however a reduction in PKCα expression was observed. Downregulation of PKCα expression/function may contribute towards the development/progression of CLL in both TCL-1 Tg mice and the PKCα-KR mouse model, similar to that noted in colon cancer models. Interestingly, PKCα expression was also reduced in the PKCα-KR mouse model, whilst GFP expression was maintained. This finding suggests that PKCα may be post-translationally targeted for degradation in CLL cells, resulting in decreased expression.[34] Results from the *in vitro* co-cultures of our model indicate that upregulated PKCβII is not required for the initiation of CLL-like cells, as $GFP^+CD19^+CD5^+$ cells were present during the early stages of the cultures, prior to PKCβII upregulation. These results suggest that loss of PKCα function may create permissive conditions for the generation of CLL, while PKCβII activation/upregulation enables disease progression. Indeed, the block in CLL development in the $PKC\beta^{-/-}$-TCL-1 Tg model may reflect the absence of both PKCβI and PKCβII in these mice.

Mouse models form an integral part of the pre-clinical development of promising therapies.[35] Due to the heterogeneity of CLL, it is important to generate models that represent the complexity of the disease. For example targeting a component of the 13q deletion incorporating the DLEU gene product in mice, present in over 50% of patients, resulted in the development of CLL.[36] In addition, the development of a CLL phenotype in Eμ-TCL-1 Tg mice has resulted in subsequent studies establishing that TCL-1 is preferentially expressed in poor prognostic patients.[37,38] Here, we demonstrate that CLL cells express lower levels of PKCα than their normal B cell counterpart suggesting that reduced expression levels of PKCα may assist in generating permissive conditions for the development of CLL. Similar to the TCL-1 Tg mouse, our model predominantly expresses unmutated IgV_H genes that exhibit longer CDR3 regions, a characteristic of poor prognostic CLL patient subsets.[39,40] While ZAP-70 was upregulated in PKCα-KR-expressing CLL-like cells to levels of at least 50% that of T cells, we were unable to detect ZAP-70 expression in splenic cells isolated from TCL-1 Tg mice, in agreement with findings reported by Gobessi *et al.*[41] However, a previous study demonstrated ZAP-70 upregulation in splenic B cells of Eμ-TCL-1 Tg mice, although the levels of expression were

significantly reduced compared with T cells.[42] The different results reported between studies may reflect the distinct techniques and antibodies used to detect ZAP-70 expression. However there does appear to be a differential amount of ZAP-70 expressed between PKCα-KR-expressing B cells and Eμ-TCL-1 Tg splenic B cells, relative to T cells which may reflect a difference in the cell of origin between these two models. These findings suggest that the two mouse models provide complementary disease systems for studying the pathogenesis of poor prognostic CLL. Notably, an advantage of the PKCα-KR model over TCL-1 Tg mouse is rapid and reliable disease onset, in a timeframe of weeks compared to months, which is beneficial when performing *in vivo* pre-clinical studies.

Although the molecular basis of CLL has not been fully understood, PKC-mediated signals control CLL survival and proliferation, and thus represent promising therapeutic targets. Enzastaurin has previously been shown to induce apoptosis in CLL cells independent of mutational status in an *in vitro* culture system.[33] Enzastaurin-mediated apoptosis has been reported to be dependent on PP2A activity.[43] Interestingly, inhibition of PKC activity by treating cells with ruboxistaurin (targeting PKCβ) or sotrastaurin (AEB071; a pan PKC inhibitor) results in the downregulation of the protein tyrosine kinase PTPN22, which plays a protective role in BCR-mediated CLL survival, leading to apoptosis *in vitro*.[44] Our studies demonstrate a selective induction of apoptosis in leukemic cells and a reduction in cellular proliferation with enzastaurin *in vitro* and *in vivo*. Enzastaurin-mediated reduction in proliferation has previously been demonstrated in a number of solid cancer models and myeloma cell lines.[45] Proliferating CLL cells are more prone to undergoing clonal evolution, which can result in the development of detrimental chromosomal abnormalities including 17p deletions that target p53, rendering the cells insensitive to first-line therapies used for CLL.[46] Indeed, upregulation of AID has been associated with elevated double strand DNA breaks in CLL cells, promoting the generation of genetic aberrations.[17] Therefore, therapies that reduce proliferation offer an important treatment option for progressive CLL. Our findings support the development of clinical studies with ruboxistaurin and sotrastaurin in CLL, given the recent promising data assessing the clinical efficacy of BCR-targeting inhibitors such as the Btk inhibitor ibrutinib.[47] In support of this, AEB071 is currently in Phase II clinical trial in diffuse large B cell lymphoma, and has recently been demonstrated to

exhibit pre-clinical activity in CLL *in vitro* and *in vivo*.[48] Targeting PKC, and in particular PKCβ, is particularly pertinent given the recent findings by Lutzny *et al.*, demonstrating that PKCβII expression in the BM stromal cells is essential for the survival and development of CLL cells.[49] Therefore inhibition of PKCβ may modify the tumor microenvironment, which is established to play a critical role in supporting CLL survival, proliferation and chemoresistance.[50]

Collectively, our results demonstrate the potential for therapeutic agents targeting PI3K/PKCβ related signaling pathways, and highlight the translational applicability of the PKCα-KR mouse model as a pre-clinical model for the development of poor prognostic CLL. Moreover, our mouse model provides a powerful tool for delineating the molecular events that occur downstream of PKCα subversion during the initiation of cellular transformation, enabling the identification of potential novel therapeutic targets for CLL.

Authorship Disclosures

RN and MV designed/performed the experiments, analyzed and interpreted the data, carried out statistical analysis and drafted the manuscript; AT, EC, KD and AH performed some experiments and carried out data analysis; AMMcC, FMcC, AGR, and JGG provided key reagents and edited the manuscript; AMM gained funding for the study, designed the research, supervised the studies, analyzed and interpreted the data and wrote the manuscript. The authors have no disclosures to declare.

References:

1. Dighiero G. CLL Biology and Prognosis. Hematology (Am Soc Hematol Educ Program) 2005;278-284.

2. Hanada M, Delia D, Aiello A, Stadtmauer E, Reed JC. bcl-2 gene hypomethylation and high-level expression in B-cell chronic lymphocytic leukemia. Blood 1993;82(6):1820-1828.

3. Messmer BT, Messmer D, Allen SL, et al. In vivo measurements document the dynamic cellular kinetics of chronic lymphocytic leukemia B cells. J Clin Invest. 2005;115(3):755-764.

4. Ghia P, Chiorazzi N, Stamatopoulos K. Microenvironmental influences in chronic lymphocytic leukaemia: the role of antigen stimulation. J Intern Med. 2008;264:549-562.

5. Herishanu Y, Pérez-Galán P, Liu D, et al. The lymph node microenvironment promotes B-cell receptor signaling, NF-kappaB activation, and tumor proliferation in chronic lymphocytic leukemia. Blood 2011;117:563-574.

6. Morilla A, Gonzalez de Castro D, Del Giudice I, et al. Combinations of ZAP-70, CD38 and IGHV mutational status as predictors of time to first treatment in CLL. Leuk Lymphoma 2008;49:2108-2115.

7. Hamblin TJ, Davis Z, Gardiner A, Oscier DG, Stevenson FK. Unmutated Ig V(H) genes are associated with a more aggressive form of chronic lymphocytic leukemia. Blood 1999;94(6):1848-1854.

8. Wiestner A, Rosenwald A, Barry TS, et al. ZAP-70 expression identifies a chronic lymphocytic leukemia subtype with unmutated immunoglobulin genes, inferior clinical outcome, and distinct gene expression profile. Blood 2003;101:4944-4951.

9. Nakagawa R, Soh JW, Michie AM. Subversion of PKCa signaling in hematopoietic progenitor cells results in the generation of a B-CLL-like population in vivo. Cancer Res. 2006;66:527-534.

10. Bichi R, Shinton SA, Martin ES, et al. Human chronic lymphocytic leukemia modeled in mouse by targeted TCL1 expression. Proc Natl Acad Sci USA 2002;99(10):6955-6960.

11. Cosimo E, McCaig AM, Carter-Brzezinski LJ, et al. Inhibition of NF-κB-mediated signaling by the cyclin-dependent kinase inhibitor CR8 overcomes prosurvival stimuli to induce apoptosis in chronic lymphocytic leukemia cells. Clin Cancer Res. 2013;19:2393-2405.

12. Soh JW, Lee EH, Prywes R, Weinstein IB. Novel roles of specific isoforms of protein kinase C in activation of the c-fos serum response element. Mol Cell Biol. 1999;19:1313-1324.

13. Nakagawa R, Mason SM, Michie AM. Determining the role of specific signaling molecules during lymphocyte development in vivo: instant transgenesis. Nat Protoc. 2006;1:1185.

14. Fallah-Arani F, Schweighoffer E, Vanes L, Tybulewicz VL. Redundant role for Zap70 in B cell development and activation. Eur J Immunol. 2008;38:1721-1733.

15. Longo PG, Laurenti L, Gobessi S, Sica S, Leone G, Efremov DG. The Akt/Mcl-1 pathway plays a prominent role in mediating antiapoptotic signals downstream of the B-cell receptor in chronic lymphocytic leukemia B cells. Blood 2008;111:846-855.

16. Palacios F, Moreno P, Morande P, et al. High expression of AID and active class switch recombination might account for a more aggressive disease in unmutated CLL patients: link with an activated microenvironment in CLL disease. Blood 2010;115:4488-4496.

17. Patten PE, Chu CC, Albesiano E, et al. IGHV-unmutated and IGHV-mutated chronic lymphocytic leukemia cells produce activation-induced deaminase protein with a full range of biologic functions. Blood 2012;120:4802-4811.

18. Abrams ST, Lakum T, Lin K, et al. B cell receptor signalling in chronic lymphocytic leukaemia cells is regulated by overexpressed active protein kinase C{beta}II. Blood 2006;109:1193-1201.

19. Alkan S, Huang Q, Ergin M, et al. Survival role of protein kinase C (PKC) in chronic lymphocytic leukemia and determination of isoform expression pattern and genes altered by PKC inhibition. Am J Hematol. 2005;79(2):97-106.

20. Goode N, Hughes K, Woodgett JR, Parker PJ. Differential regulation of glycogen synthase kinase-3 beta by protein kinase C isotypes. J Biol Chem. 1992;267:16878-16882.

21. Griner EM, Kazanietz MG. Protein kinase C and other diacylglycerol effectors in cancer. Nat Rev Cancer 2007;7:281-294.

22. Michie AM, Nakagawa R. The link between PKCa regulation and cellular transformation. Immunol Letts. 2005;96:155-162.

23. Tan M, Li P, Sun M, Yin G, Yu D. Upregulation and activation of PKC alpha by ErbB2 through Src promotes breast cancer cell invasion that can be blocked by combined treatment with PKC alpha and Src inhibitors. Oncogene 2006;25:3286-3295.

24. Lønne GK, Cornmark L, Zahirovic IO, Landberg G, Jirström K, Larsson C. PKCalpha expression is a marker for breast cancer aggressiveness. Mol Cancer 2010;9:76.

25. Alvaro V, Prevostel C, Joubert D, Slosberg E, Weinstein BI. Ectopic expression of a mutant form of PKCalpha originally found in human tumors: aberrant subcellular translocation and effects on growth control. Oncogene 1997;14(6):677-685.

26. Neill GW, Ghali LR, Green JL, Ikram MS, Philpott MP, Quinn AG. Loss of protein kinase Calpha expression may enhance the tumorigenic potential of Gli1 in basal cell carcinoma. Cancer Res. 2003;63:4692-4697.

27. Tibudan SS, Wang Y, Denning MF. Activation of protein kinase C triggers irreversible cell cycle withdrawal in human keratinocytes. J Invest Dermatol. 2002;119:1282-1289.

28. Detjen KM, Brembeck FH, Welzel M, et al. Activation of protein kinase Calpha inhibits growth of pancreatic cancer cells via p21(cip)-mediated G(1) arrest. J Cell Sci. 2000;113:3025-3035.

29. Gökmen-Polar Y, Murray NR, Velasco MA, Gatalica Z, Fields AP. Elevated protein kinase C betaII is an early promotive event in colon carcinogenesis. Cancer Res. 2001;61:1375-1381.

30. Oster H, Leitges M. Protein kinase C alpha but not PKCzeta suppresses intestinal tumor formation in ApcMin/+ mice. Cancer Res. 2006;66:6955-6963.

31. Leitges M. Functional PKC in vivo analysis using deficient mouse models. Biochem Soc Trans. 2007;35:1018-1020.

32. Murray NR, Davidson LA, Chapkin RS, Clay Gustafson W, Schattenberg DG, Fields AP. Overexpression of protein kinase C betaII induces colonic hyperproliferation and increased sensitivity to colon carcinogenesis. J Cell Biol. 1999;145:699-711.

33. Holler C, Piñón JD, Denk U, et al. PKCbeta is essential for the development of chronic lymphocytic leukemia in the TCL1 transgenic mouse model: validation of PKCbeta as a therapeutic target in chronic lymphocytic leukemia. Blood 2009;113:2791-2794.

34. Leontieva OV, Black JD. Identification of two distinct pathways of protein kinase Calpha down-regulation in intestinal epithelial cells. J Biol Chem. 2004;279(7):5788-5801.

35. Blyth K, Morton JP, Sansom OJ. The right time, the right place: will targeting human cancer-associated mutations to the mouse provide the perfect preclinical model? Curr Opin Genet Dev. 2012;22:28-35.

36. Klein U, Lia M, Crespo M, et al. The DLEU2/miR-15a/16-1 cluster controls B cell proliferation and its deletion leads to chronic lymphocytic leukemia. Cancer Cell 2010;17:28-40.

37. Johnson AJ, Lucas DM, Muthusamy N, et al. Characterization of the TCL-1 transgenic mouse as a preclinical drug development tool for human chronic lymphocytic leukemia. Blood 2006;108(4):1334-1338.

38. Herling M, Patel KA, Khalili J, et al. TCL1 shows a regulated expression pattern in chronic lymphocytic leukemia that correlates with molecular subtypes and proliferative state. Leukemia 2006;20(2):280-285.

39. Fais F, Ghiotto F, Hashimoto S, et al. Chronic lymphocytic leukemia B cells express restricted sets of mutated and unmutated antigen receptors. J Clin Invest. 1998;102(8):1515-1525.

40. Yan XJ, Albesiano E, Zanesi N, et al. B cell receptors in TCL1 transgenic mice resemble those of aggressive, treatment-resistant human chronic lymphocytic leukemia. Proc Natl Acad Sci USA 2006;103(31):11713-11718.

41. Gobessi S, Belfiore F, Bennardo S, Doe B, Laurenti L, Efremov DG. Expression of ZAP-70 does not accelerate leukemia development and progression in the Emu-TCL1 transgenic mouse model of chornic lymphocytic leukemia. 54th ASH Annual Meeting Abstract 2012;641:925.

42. Sanchez-Aguilera A, Rattmann I, Drew DZ, et al. Involvement of RhoH GTPase in the development of B-cell chronic lymphocytic leukemia. Leukemia 2010;24(1):97-104.

43. Liffraud C, Quillet-Mary A, Fournié JJ, Laurent G, Ysebaert L. Protein phosphatase-2A activation is a critical step for enzastaurin activity in chronic lymphoid leukemia cells. Leuk Lymphoma 2012;53:966-972.

44. Negro R, Gobessi S, Longo PG, et al. Overexpression of the autoimmunity-associated phosphatase PTPN22 promotes survival of antigen-stimulated CLL cells by selectively activating AKT. Blood 2012;119:6278-6287.

45. Neri A, Marmiroli S, Tassone P, et al. The oral protein-kinase C beta inhibitor enzastaurin (LY317615) suppresses signalling through the AKT pathway, inhibits proliferation and induces apoptosis in multiple myeloma cell lines. Leuk Lymphoma 2008;49:1374-1383.

46. Stilgenbauer S, Sander S, Bullinger L, et al. Clonal evolution in chronic lymphocytic leukemia: acquisition of high-risk genomic aberrations associated with unmutated VH, resistance to therapy, and short survival. Haematologica 2007;92:1242-1245.

47. Byrd JC, Furman RR, Coutre SE, et al. Targeting BTK with ibrutinib in relapsed chronic lymphocytic leukemia. N Engl J Med. 2013;369:32-42.

48. El-Gamal D, Williams K, LaFollette TD, et al. PKC-β as a therapeutic target in CLL: PKC inhibitor AEB071 demonstrates preclinical activity in CLL. Blood 2014;124(9):1481-1491.

49. Lutzny G, Kocher T, Schmidt-Supprian M, et al. Protein Kinase C-b-Dependent Activation of NF-kB in Stromal Cells Is Indispensable for the Survival of Chronic Lymphocytic Leukemia B Cells In Vivo. Cancer Cell 2013;23:77-92.

50. Ten Hacken E, Burger J. Molecular Pathways: Targeting the microenvironment in chronic lymphocytic leukemia- focus on the B cell receptor. Clin Cancer Res. 2014;20:548-556.

Sample No.	V_H gene	J_H gene	D_H gene	Similarity to germline (%)	Mutation status	CDR3 length
MIEV-1	IGHV1-9*01	IGHJ4*01	IGHD2-3*01	99.7	UM	14
MIEV-2	IGHV1S20*02	IGHJ2*01	IGFD1-1*01	98.6	UM	11
MIEV-3	IGHV1S132*01	IGFJ4*01	IGHD1-1*02	98.6	UM	13
MIEV-4	IGV5-4*02	IGHJ3*01	IGHD4-1*01	97.1	M	11
MIEV-5	IGHV1S15*01	IGHJ3*01	IGHD2-3*01	98.3	UM	9
MIEV-6	IGHV14-1*01	IGHJ3*01	IGHD2-12*01	97.1	M	13
MIEV-7	IGHV1-63*02	IGHJ1*01	IGHD2-1*01	97.1	M	11
MIEV-8	IGHV1-9*01	IGHJ4*01	IGHD2-3*01	97.6	M	14
PKCα-KR-1	IGHV1-39*01	IGHJ4*01	IGHD2-1*01	98.6	UM	12
PKCα-KR-2	IGV1S20*02	IGHJ2*01	IGHD1-1*01	93.3	M	14
PKCα-KR-3	IGHV1-63*02	IGHJ4*01	IGHD3-2*02	97.1	M	14
PKCα-KR-4	IGHV1-39*01	IGHJ4*01	IGHD2-1*01	100	UM	12
PKCα-KR-5	IGHV1-69*02	IGHJ1*03	IGHD1-1*01	98.9	UM	16
PKCα-KR-6	IGHV1-23*01	IGHJ1*01	IGHD1-1*01	99.3	UM	13
PKCα-KR-7	IGHV14-4*01	IGHJ3*01	IGHD1-1*01	99	UM	14
PKCα-KR-8	IGHV81*01	IGHJ2*01	IGHD2-1*01	99	UM	13

Table 1: Summary of IgV_H rearrangements generated in mice transplanted with MIEV- or PKCα-KR-expressing cells. GFP^+ leukemic B cells generated *in vivo*, were isolated prior to cloning and sequencing of IgV_H regions. Sequences were analyzed using IMGT (www.imgt.org). In-frame sequences are shown.

Figure Legends.

Figure 1. PKCα-KR-expressing cells phenotypically resemble human CLL cells by surface protein expression. (**A**) MIEV- or PKCα-KR-HPC-OP9 co-cultures were analyzed by flow cytometry at d10. FACS plots shown are live and size (FSC/SSC) and haemopoietic lineage ($CD45^+$) gated prior to analysis for CD5 vs. CD19, CD23 vs. CD19 and IgM vs. CD19 as indicated. Percentages are indicated in the corner of the quadrants. (**B**) The mean fluorescence intensity (MFI) of CD19, CD5, CD23 and IgM was calculated for a minimum of 3 individual biological replicates. Data is represented as mean (± SEM). p values were generated using a student's unpaired t-test to compare groups (*$p<0.05$; **$p<0.005$; ***$p<0.001$). (**C**) A histogram comparing the surface expression of CD23 on $GFP^+CD45^+CD19^+CD5^+$-gated MIEV or PKCα-KR cells, against relative cell number (RCN).

Figure 2. CLL-like cells disseminate into primary and secondary lymphoid organs. MIEV- and PKCα-KR-HPCs were i.p. injected into RAG-$1^{-/-}$ neonates. (**A**) Kaplan-Meier curves comparing the survival rates in mice adoptively-transferred with MIEV-HPCs (500K-pale grey line, square (n=5)) or PKCα-KR-HPCs (500K-mid-grey line, triangle (n=5); 300K-dark grey line, circle (n=6); 100K-dotted line (n=4)). Log-rank (Mantel-Cox) test found an overall significant difference was found ($p=0.0013$). The log-rank test of trend revealed a significant linear trend between the number of cells injected and the survival of mice ($p=0.0001$). (**B**) Spleen weights from $RAG^{-/-}$, MIEV-HPC and PKCα-KR-HPC mice are shown as a percentage of total body weight. Student's unpaired t-test was performed; * $p<0.05$. The graphs were generated from 6 spleens per condition. (**C**) 5 wk post reconstitution mice were sacrificed. Paraffin-embedded spleens from $RAG^{-/-}$ host mice (top) MIEV (middle) or PKCα-KR (bottom) were sectioned and stained with either H&E (left) or anti-B220 antibody (brown; right). 4 x magnification shown. (**D**) Single cell suspension were prepared from organs as indicated and analyzed by flow cytometry for CLL cell markers, CD19 and CD5 after live and size (FSC/SSC) and GFP^+CD45^+ gating. (**E**) The percentage of GFP^+CD19^+ cells or $GFP^+CD19^+CD5^+$ cells within total hematopoietic $CD45^+$ cells in the indicated organs is shown for mice reconstituted with MIEV- or PKCα-KR-HPCs as indicated. Student's unpaired t-test was

performed; * $p<0.05$, ** $p<0.005$, ***$p<0.001$. The graphs were generated from 10 individual mice.

Figure 3. PKCα-KR-transduced CLL-like cells resemble poor prognostic CLL patient samples. (**A**) MIEV- or PKCα-KR-HPCs were analyzed by flow cytometry for intracellular levels of ZAP-70 at d12 of co-culture. Solid line, PKCα-KR; dotted line, MIEV; shaded, isotype control. A representative blot of 3 independent cultures is shown. (**B**) The percentage of ZAP-70^+ cells was analyzed by flow cytometry in B lineage cells isolated from the spleens of ICR-WT, Eμ-TCL-1 Tg and PKCα-KR-HPC mice. Isotype and ICR-T cell positive controls are shown. (**C**) Protein lysates were prepared from MIEV-FL or PKCα-KR-FL co-cultures at d10 and d16. Western blots were carried out, immunoblotting for phosphorylated and total ERK1/2, phosphorylated and total S6, and an additional loading control, GAPDH. (**D**) Proliferation was assessed by culturing 50,000 MIEV- or PKCα-KR cells from early (d6 – d10) and late (d15 – d20) stages of the cultures and incubating cells with BrdU for 2 hr prior to the end of the 24 hr timepoint. Data are represented as mean (± SEM) of at least 3 biological replicates, each carried out in technical triplicates. (**E**) Ki-67 expression levels (MFI) were analyzed in CD19-MACS-purified ICR-WT and PKCα-KR-HPC spleens. (**F**) RNA was isolated from MIEV- or PKCα-KR-OP9 cells derived from early (d6 – d10) and late (d15 – d20) stages of the cultures and subjected to qRT-PCR to evaluate the levels of *aicda* expression. Results are expressed as $2^{(-_{\Delta\Delta}CT)}$ relative to GAPDH reference gene. Data are represented as mean (± SEM) of at least 3 biological replicates, each carried out in technical triplicates. Student's unpaired t-test was performed; * $p<0.05$, ** $p<0.005$.

Figure 4. CLL cells isolated from mouse models and CLL patient samples exhibit altered PKC isoform expression profiles. (**A**) Protein lysates were prepared from MIEV- or PKCα-KR-HPC derived cells at the indicated times, separated by gel electrophoresis and immunoblotted for PKC substrates using the anti-phospho-Ser PKC substrate antibody (pSer-PKC-substrate). GAPDH was included as a protein loading control. (**B**) Protein kinase assay was carried out on cells prepared from d17 MIEV- or PKCα-KR-OP9 co-cultures. Student's unpaired t-test was performed; * $p<0.05$. (**C**) Protein lysates were prepared from MIEV- or PKCα-KR-OP9 co-cultures

and immunoblotted for PKCβI, PKCβII and GAPDH as a protein loading control. (**D**) Protein lysates were prepared from earlier and later MIEV- or PKCα-KR-OP9 co-cultures as indicated and immunoblotted for PKCβII and GAPDH as a protein loading control. (**E**) Protein lysates were prepared from B lineage cells of freshly isolated peripheral blood samples derived from healthy donors or CLL patients. Membranes were immunoblotted for PKCα, PKCβII and GAPDH as a protein loading control. (**F**) Protein lysates were prepared from MACS-isolated spleen B cells from age-matched C57BL/6 (n=5), Eμ-TCL-1 Tg (n=5) and PKCα-KR-expressing (n=4) mice and immunoblotted for PKCα, PKCβII and GAPDH as a protein loading control. A representative blot (left) and the mean expression (±SEM) of PKCα (left) and PKCβII (right) as a ratio of GAPDH are shown. (**G**) Protein lysates were prepared from MACS-isolated spleen B cells of Eμ-TCL-1 Tg (n=5), PKCα-KR-expressing (n=4) and age-matched C57BL/6 (n=5) mice and immunoblotted for pERK/ERK and pS6/S6. A representative blot (left) and the mean expression (±SEM) of pERK as a ratio of ERK (left) and pS6 as a ratio of S6 (right) are shown.

Figure 5. Enzastaurin induced cell cycle arrest and apoptosis in CLL-like cells. MIEV- or PKCα-KR-HPC-derived cells were cultured for 24 hr in the presence of enzastaurin (ENZA) as indicated. (**A**) Protein lysates were prepared from late co-cultures (post-d15) of MIEV- or PKCα-KR-expressing cells. Proteins separated by gel electrophoresis and immunoblotted for phospho-GSK3β^{S9}, GSK3β and tubulin as a protein loading control. Densitometry was performed on the blots, assessing the phospho-GSK3β^{S9} signal compared with GSK3β signal strength. The mean percentage (± SEM) of phospho-GSK3β signal reduction of untreated cells from 3 independent experiments is shown. (**B**) Flow cytometry was used to assess the level of apoptosis induced upon enzastaurin treatment of MIEV- vs. PKCα-KR cells and splenic B lineage cells isolated from age-matched C57BL/6 vs. Eμ-TCL-1 transgenic mice. Annexin V$^+$DAPI$^-$ cells represent early apoptotic cells. Data are represented as mean (± SEM) of 3 biological replicates. (**C**) PI analysis was used to calculate the phases of the cell cycle (G_0/G_1 and G_2M shown). Data shown excludes the sub-G_0 population. Data are represented as mean (± SEM) of at least 3 biological replicates. Open circle - PKCα-KR; filled circle - MIEV. (**D**) MIEV- or PKCα-KR-expressing cells were cultured for 24 or 48 hr in the presence of ENZA, as indicated. Cells were

incubated with BrdU for 2 hr prior to the end of the timepoint. Absorbance values were read at 492 nm to 370 nm after addition of TMB substrate. Data shown are the mean (± SEM) of at least 3 biological replicates, each carried out in technical triplicates. p values were generated using the student's unpaired t-test * $p<0.05$, ** $p<0.005$, *** $p<0.001$.

Figure 6. Enzastaurin reduced leukemic burden and selectively induced apoptosis in CLL-like cells *in vivo*. CLL-like diseased mice were generated by adoptively transferring $4x10^5$ PKCα-KR-FL cells into RAG-$1^{-/-}$ neonates. 4 - 6 wk post injection, on confirmation of a population of CLL-like cells in the blood (≥ 0.4%), mice were dosed with either ENZA or vehicle control (D5W) for up to 21 days. Thereafter, blood, BM, spleen and LN were analyzed for leukemic burden and level of apoptosis by flow cytometry as indicated. (**A**) Representative flow cytometric analysis of vehicle- or ENZA-treated mice. Data shown are analyzed for CLL cell markers, CD19 and CD5 after live and size (FSC/SSC), GFP^+ and $CD45^+$ gating. The percentage of GFP^+ CLL-like cells within the total population is shown. (**B**) Percentage (left) and number (right) of $GFP^+CD45^+CD19^+$ $CD5^+$ population is shown in the ENZA-treated and D5W mice in the organs indicated. (**C**) Percentage of $GFP^+CD45^+CD19^+$ $CD5^+$ cells in the blood in pre-, during, and post-ENZA-treated and vehicle-treated mice. (**D**) Percentage of Annexin V^+7-AAD^- apoptosing cells was calculated within the GFP^+CD19^+ population of ENZA- and vehicle-treated mice. All data shown is the mean (± SEM) of 6 individual mice. p values were generated using the student's unpaired t-test * $p<0.05$, ** $p<0.005$.

Figure 1 - Nakagawa *et al.*,

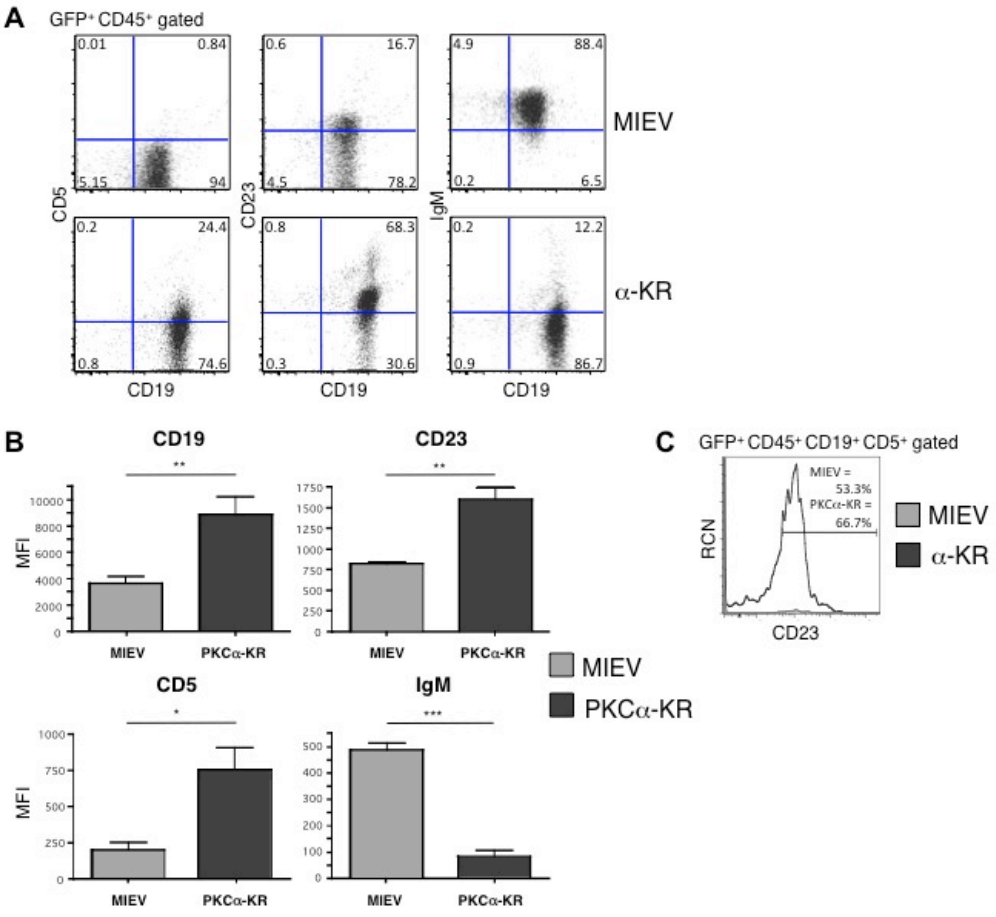

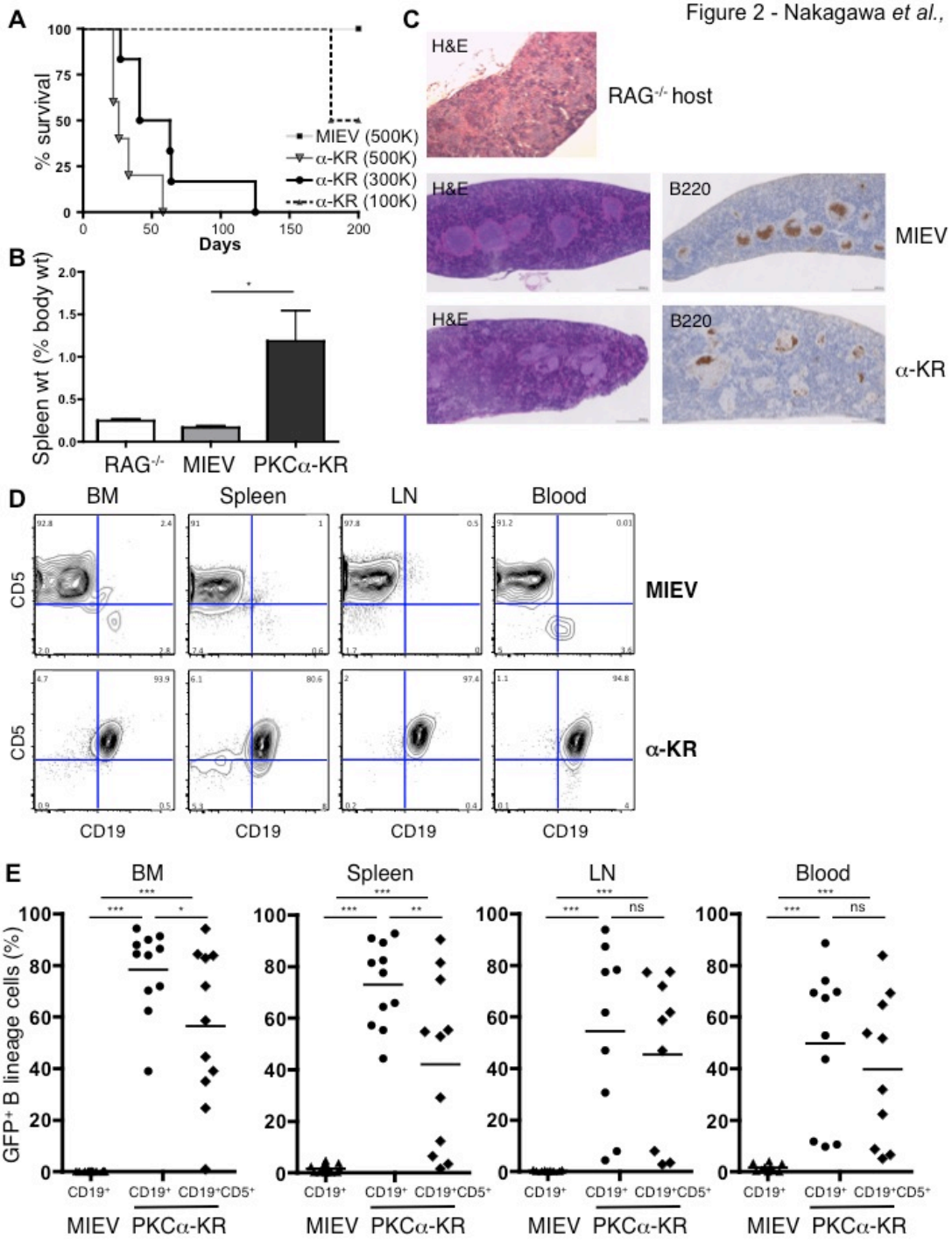
Figure 2 - Nakagawa et al.,
A
% survival
Days
MIEV (500K)
α-KR (500K)
α-KR (300K)
α-KR (100K)
B
Spleen wt (% body wt)
RAG-/-
MIEV
PKCα-KR
C
H&E
RAG-/- host
B220
MIEV
α-KR
D
BM
Spleen
LN
Blood
CD5
CD19
MIEV
α-KR
E
GFP+ B lineage cells (%)
CD19+
CD19+CD5+
MIEV
PKCα-KR
ns

Figure 3 - Nakagawa *et al.*,

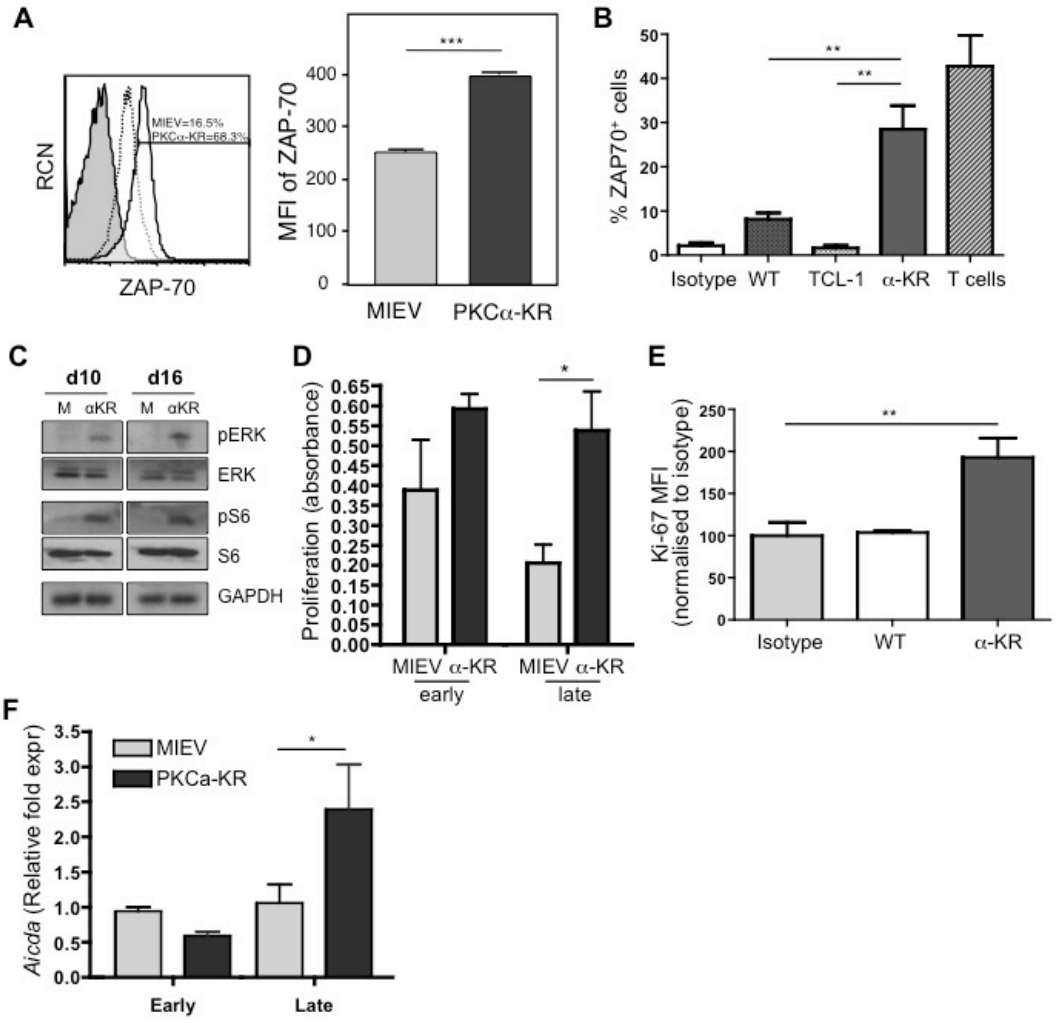

Figure 4 - Nakagawa *et al.*,

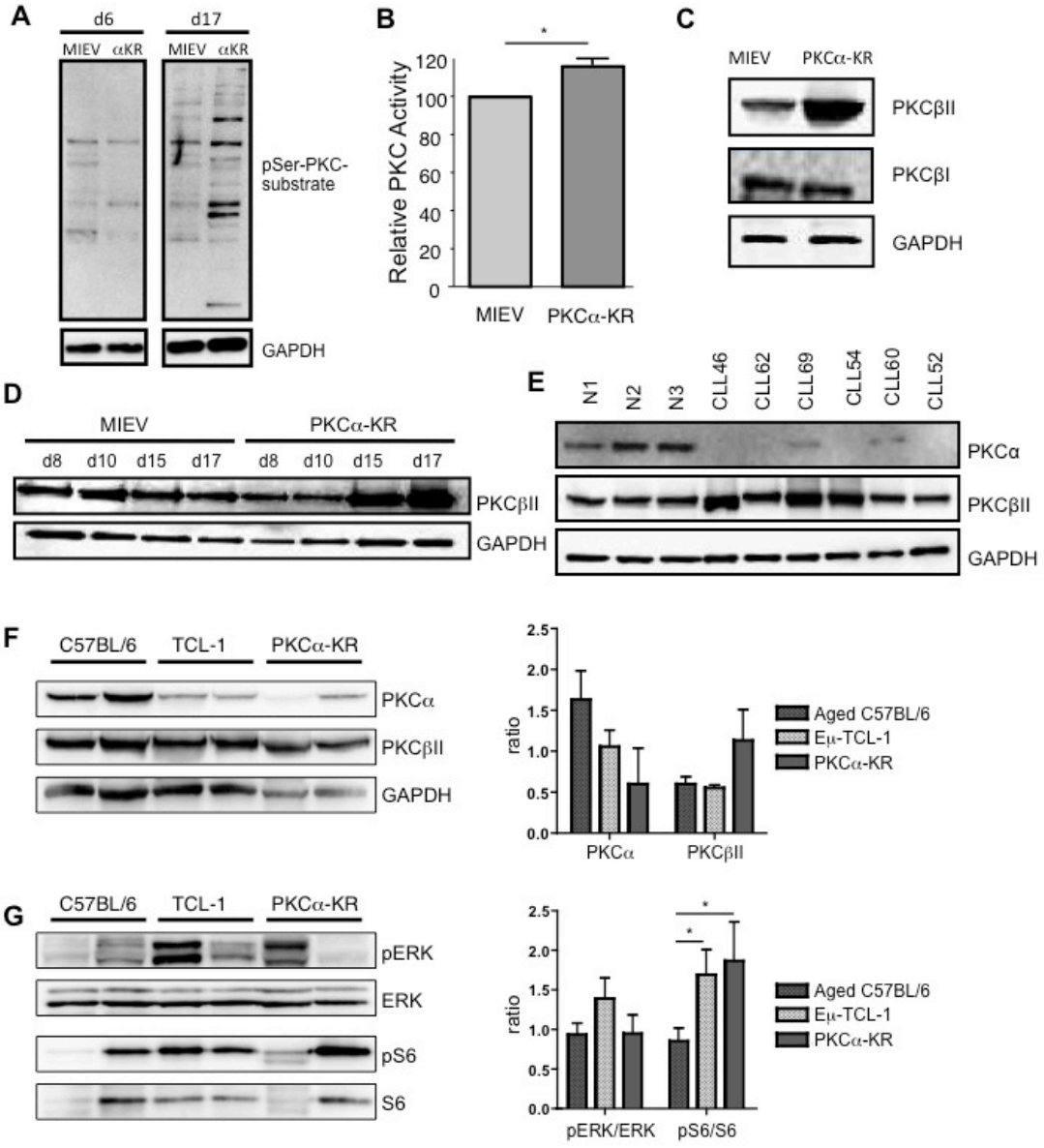

Figure 5 - Nakagawa *et al.*,

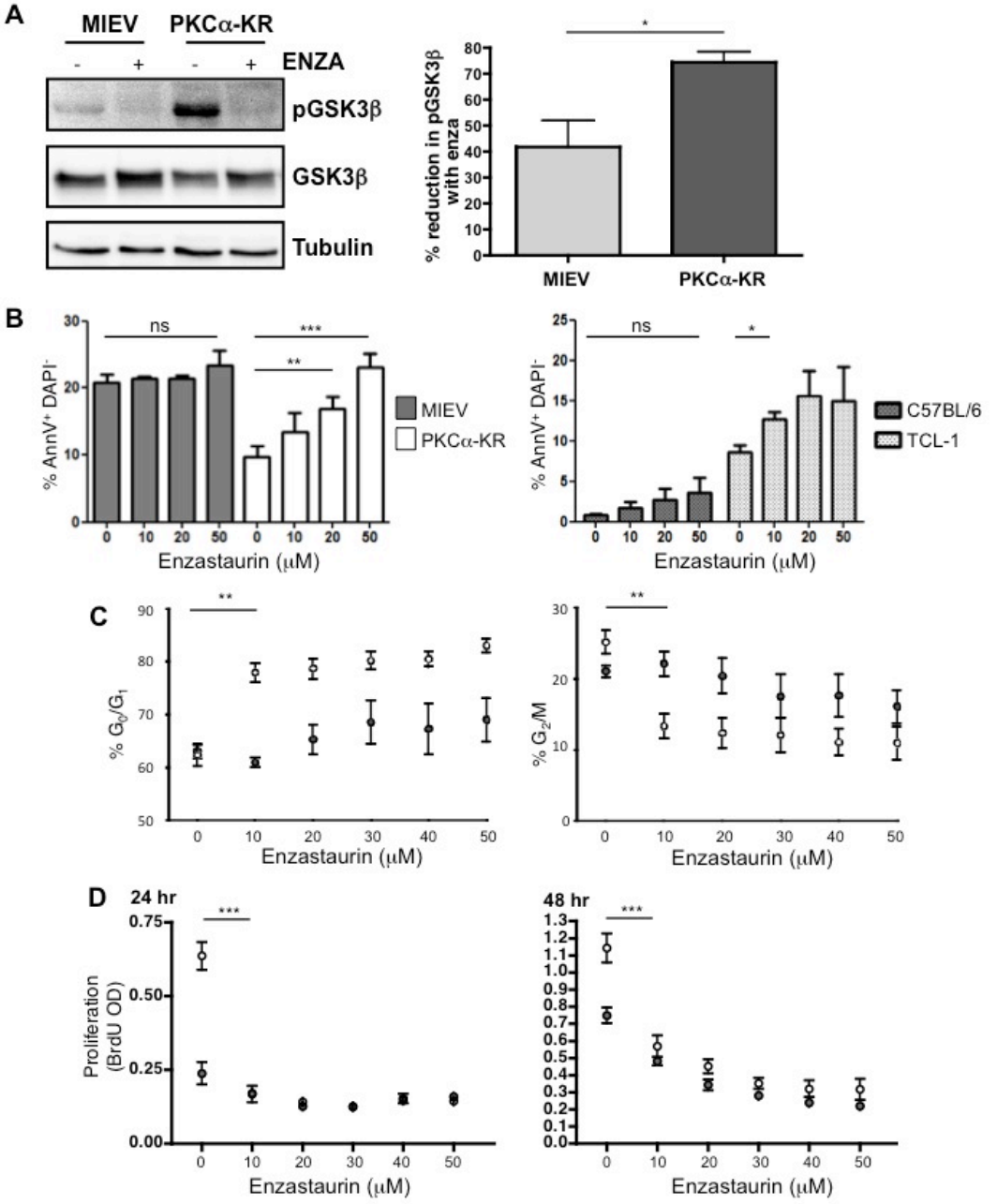

Figure 6 - Nakagawa *et al.*,

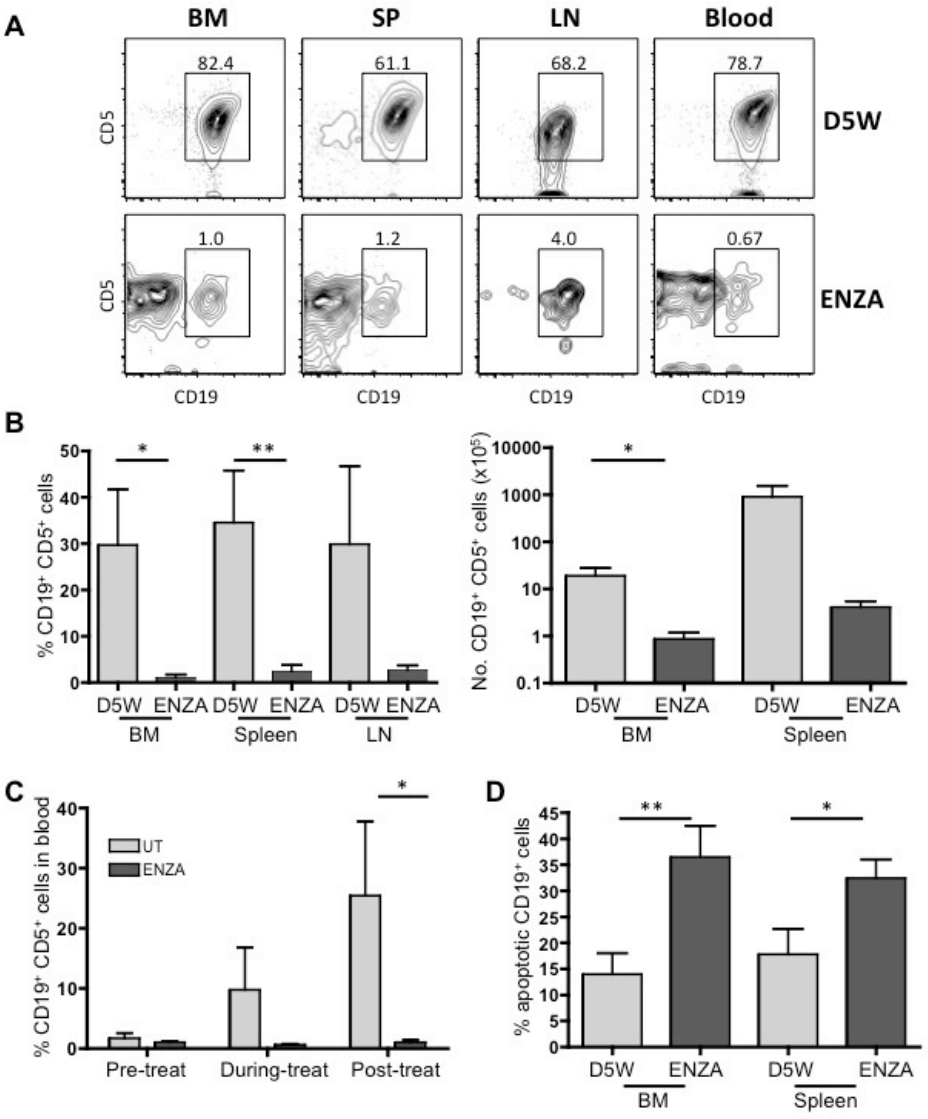

Supplementary Methods

Flow Cytometric Analysis. Combinations of anti-CD23-PE (B3B4), anti-CD45-PerCP (30-F11), anti-IgM-PE-Cy7 (R6-60.2), anti-CD5-APC (53-7.3) and anti-CD19-APC-Cy7 (1D3) were used. For ZAP-70 intracellular staining, surface CD19 staining was followed by fixation with cytofix/cytoperm (BD Biosciences). The ZAP-70 antibody was either directly-conjugated with PE (1E7.2) or purified (clone 29) and detected by PE-conjugated goat anti-mouse IgG antibody. Mouse IgG2a isotype was used for control staining.

Histology and immunohistochemistry. For histological analysis, 3-μm sections were stained with haematoxylin and eosin (H&E) with a standard protocol (Glasgow Royal Infirmary, UK). For immunohistochemical staining, paraffin-embedded sections were dehydrated with xylene and ethanol then antigenic epitopes were exposed by using an EDTA solution (10 mM Tris/1 mM EDTA, pH 8.0) and microwaving. Endogenous biotin was blocked with avidin/biotin blocking kit (Vector Labs, Peterborough, UK), and sections were blocked with peroxidase blocking solution (3% H_2O_2). Thereafter, sections were blocked with 5% horse serum then stained with biotin-conjugated anti-B220 antibody (clone RA3-6B2), detected by HRP-Vectastain ABC kit (Dako, Ely, UK) and ImmPACTTM diaminobenzidine.

Determine the mutational status of IgV_H. GFP^+ splenic cells were isolated by cell sorting on a FACSAriaI (BD Biosciences), RNA was extracted using the RNAeasy kit (Qiagen, Manchester UK) and reverse transcribed with AMV (Roche Diagnostics) using oligo(dT)15 primers. cDNA was amplified with PCR primer combinations and cycles as described previously.[1] PCR products were cloned into pCRII-Blunt-TOPO (Invitrogen) and sequenced with M13 reverse/forward primers.

Western Blotting. Protein lysates containing equal protein amounts from MIEV- or PKCα-KR-HPC-co-cultures were separated by SDS-PAGE and transferred onto PVDF membrane, and blocked as described previously.[2] All antibodies were obtained from Cell Signaling Technologies (Danvers, MA) except anti-$PKC\beta_I$ (E-3) and anti-$PKC\beta_{II}$ (sc-210) antibodies, which were obtained from Santa Cruz Biotechnology

(Santa Cruz, CA). The blots were developed with Immun-Star™ Western C™ HRP chemiluminescence kit.

1. White HN. Restriction-PCR fingerprinting of the immunoglobulin VH repertoire: direct detection of an immune response and global analysis of B cell clonality. Eur J Immunol. 1998;28:3268-3279.

2. Nakagawa R, Vukovic M, Cosimo E, Michie AM. Modulation of PKC-α promotes lineage reprogramming of committed B lymphocytes. Eur J Immunol. 2012;42:1005-1015.

CLL sample ID	Treated	Sex	Stage[a]	ZAP-70 status[b]	IgV_H Mutational status[c]	Cytogenetics	PKCα expression[d] (rel to normal B)
14	Y	M	C	Pos		17p del	High
23	N	F	A		UM		High
32	N	F	B	Pos	UM	Normal	Low
34	Y	M	B	Pos	UM	11q del	NE
41	N	M	A	Neg		Normal	NE
45	Y	M	B	Pos	UM	13q del	NE
46	N	F	A	Pos	M	Normal	NE
51	N	M	A	Neg	M	Normal	Same
52	Y	F	B	Neg	M	11q del	NE
54	N	F	A	Neg	M	Normal	NE
56	N	F	A				NE
58	N	M	A				NE
60	N	F	A	Pos	M	Normal	low
62	Y	F	A		M		NE
69	Y	M	A	Pos	UM	Normal	low
70	N	F	C	Neg		Normal	Same

Table S1. Summary of the clinical parameters of the CLL samples and PKCα expression levels.

[a] CLL disease stage according to Binet staging.

[b] ZAP-70 analysis was conducted by immunohistochemistry in the regional haematology laboratory.

[c] IgV_H is considered mutated when there is a deviation of >2% from the germline sequence.

[d] PKCα expression was determined by Western blotting, and compared with expression of normal B cells isolated from PBMCs. NE – no expression detected.

Figure S1 - Nakagawa *et al.*,

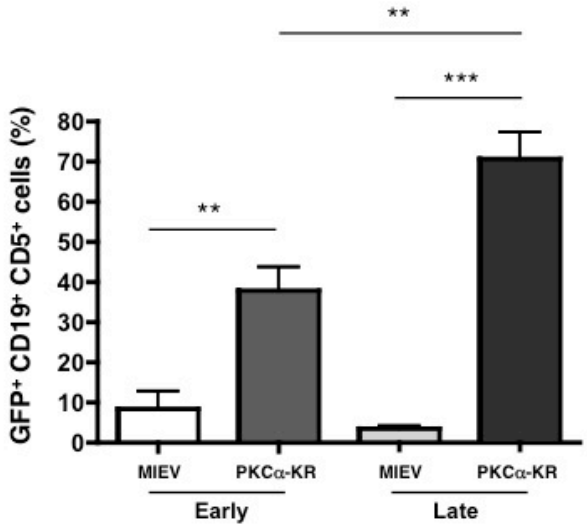

Figure S1. The percentage of the CLL-like CD19$^+$CD5$^+$ population increases over time in the PKCα-KR cocultures. HPC-OP9 co-cultures were analysed by flow cytometric analysis at early (d6 – d10) and late (d15 – d21) stages of the co-culture. The plots shown are live and size (FSC/SSC) gated and additionally gated for haemopoietic (CD45$^+$), PKCα-KR (GFP$^+$) and CLL-like (CD19$^+$CD5$^+$) cells. Student's unpaired t-test was performed; ** $p<0.005$; *** $p<0.001$. The graphs were generated from at least 5 individual experiments.

Figure S2 - Nakagawa *et al.*,

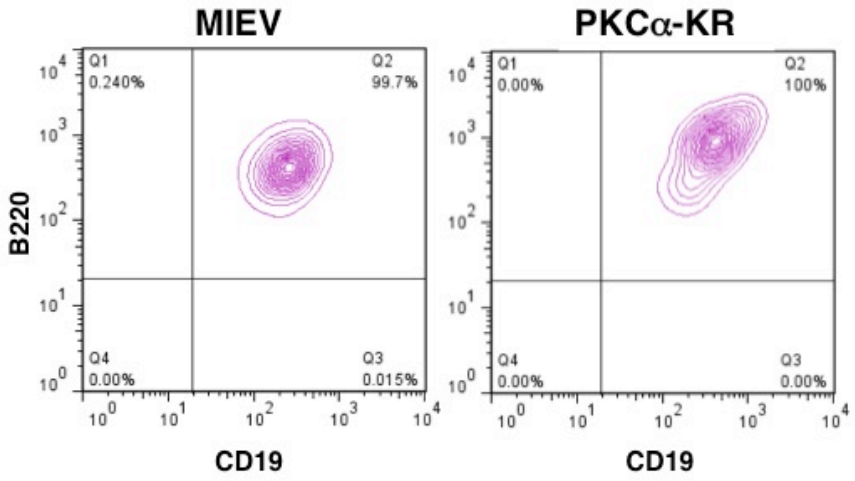

Figure S2. B lineage cells derived from MIEV- and PKCα-KR-transduced cells co-stain for CD19 and B220. HPC-OP9 co-cultures were analysed by flow cytometric analysis. The plots shown are live and size (FSC/SSC) gated and additionally gated for haemopoietic ($CD45^+$) cells.

Figure S3 - Nakagawa *et al.*,

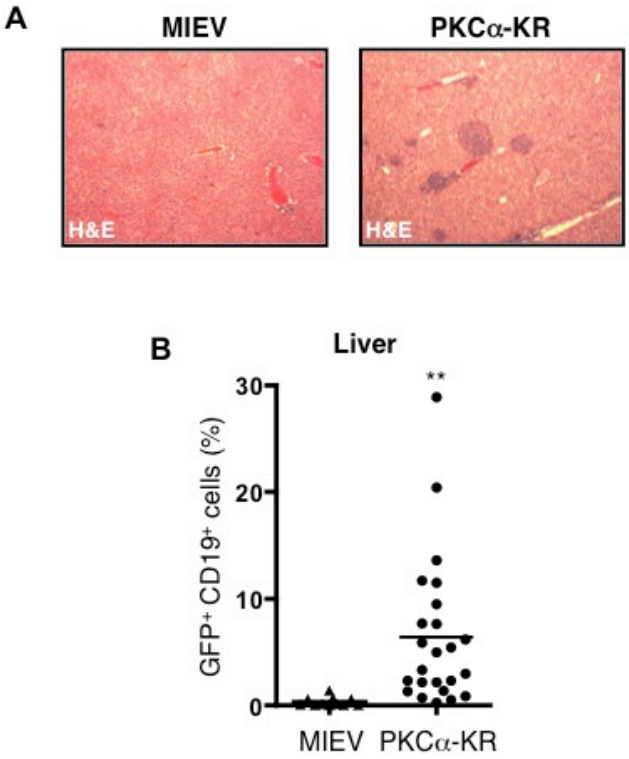

Figure S3. CLL-like cells infiltrate the liver of adoptively-transferred mice. MIEV- and PKCα-KR-transduced HPCs were i.p. injected into RAG-1$^{-/-}$ neonates. After 5 wk the reconstituted mice were sacrificed and the liver was isolated. (**A**) Paraffin-embedded spleens from MIEV (left) or PKCα-KR (right) were sectioned and stained with H&E. x 4 magnification shown. (**B**) The percentage of GFP$^+$CD19$^+$ cells within total hematopoetic CD45$^+$ cells in the liver is shown for mice reconstituted with MIEV- or PKCα-KR-HPCs. Student's unpaired t-test was performed; ** $p<0.005$. The graphs were generated from at least 10 individual mice.

Figure S4 - Nakagawa *et al.*,

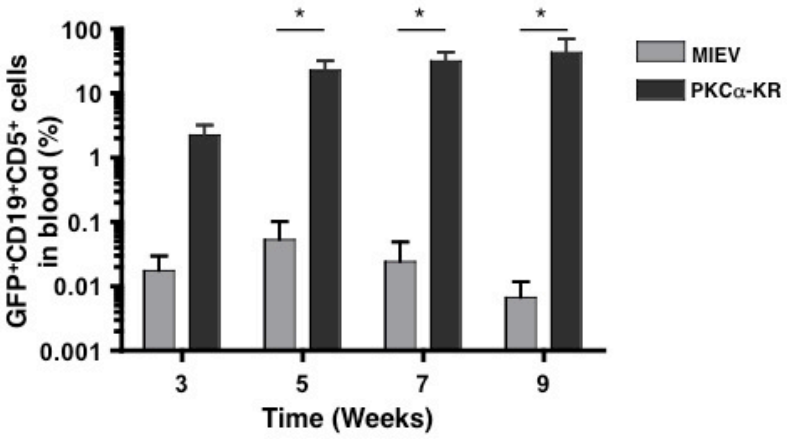

Figure S4. The percentage of the CLL-like CD19$^+$CD5$^+$ cells increases over time in the blood of PKCα-KR-HPC adoptively-transferred mice. MIEV- and PKCα-KR-transduced HPCs were i.p. injected into RAG-1$^{-/-}$ neonates. The blood was sampled 3 – 9 wk post injection and stained with CLL markers for flow cytometry. The population percentage was assessed by live and size (FSC/SSC) gating and the percentage of PKCα-KR (GFP$^+$) and CLL-like (CD19$^+$CD5$^+$) cells within the CD45$^+$ cells is shown. Student's unpaired t-test was performed; * $p<0.05$. Each data point is generated from 3 - 5 individual mice.

Figure S5 - Nakagawa *et al.*,

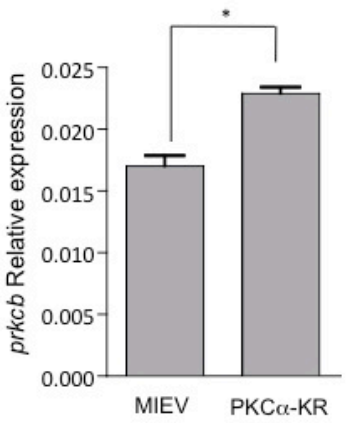

Figure S5. CLL cells isolated from the PKCα-KR mouse model exhibit altered PKCβ expression. RNA was isolated from d17 MIEV- or PKCα-KR-OP9 co-cultures and subjected to qRT-PCR to evaluate the levels of *PRKCB* expression. Results are expressed as $2^{(-\Delta CT)}$ relative to GAPDH reference gene and represent mean ± SEM (* $p<0.05$).

Figure S6 - Nakagawa *et al.*,

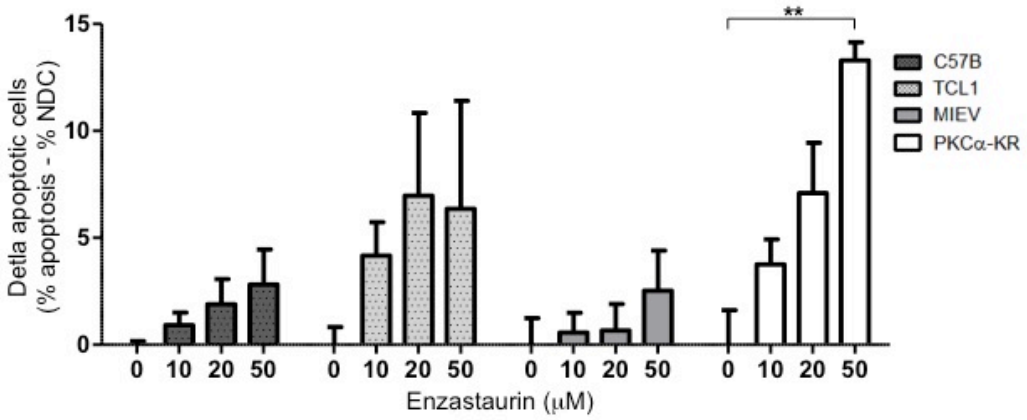

Figure S6. Enzastaurin selectively induces apoptosis in PKCα-KR-expressing CLL-like cells. Flow cytometry was used to assess the level of apoptosis induced upon enzastaurin treatment of MIEV- vs. PKCα-KR cells and splenic B lineage cells isolated from age-matched C57BL/6 vs. Eμ-TCL-1 transgenic mice. Annexin V^+DAPI^- cells represent early apoptotic cells. Data show the percentage of Annexin V^+DAPI^- cells after subtraction of background apoptosis (cells cultured in the absence of enzastaurin (0), and is referred to as the "delta apoptotic cells". Data shown are the mean (± SEM) of 3 biological replicates (** $p<0.01$).